Supplemental Data. Szydlowski et al. (2009) Starch granule initiation in *Arabidopsis* requires the presence of either Class IV or Class III starch synthases.

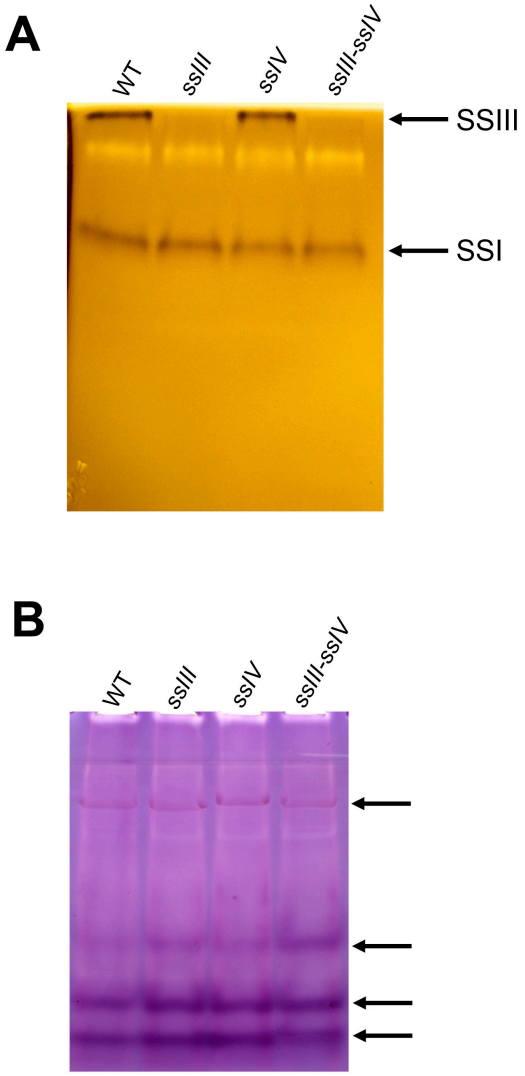

Supplemental Figure 1. **Starch synthase and phosphoglucomutase activity of *sslII-sslV* double mutant using native PAGE**. Leaves from wild-type, and *sslII*, *sslV*, and *sslII-sslV* mutant plants were used to prepare crude extracts as described in the Materials and Methods section: 150 µg of total protein was loaded in each lane. **A)** Detection of starch synthase isoforms in glycogen-containing gels. After electrophoresis, the gel was incubated overnight in a medium containing 2 mM ADP-glucose and then stained with iodine solution to reveal dark bands where starch synthase had elongated linear chains. Only bands corresponding to SSI and SSIII activities are visible with this technique. **B)** Detection of phosphoglucomutase activity. After migration the gel was incubated at room temperature in the following buffer: Tris/HCl 200 mM pH 7.0, EDTA 1 mM, MgCl2 50 mM, glucose-1-phosphate 15 mM, NAD 0.5 mM, NADP 0.25 mM, glucose-1,6-diphosphate 0.05 mM, 17 units of glucose-6-phosphate deshydrogenase, 3-(4,5-dimethylthiazol)-2,5 diphenyltetrazolium bromide (MTT), 1 mM, 5-methyl- phenazinium methyl sulfate (PMS) 0.5 mM. The reaction was stopped after incubation for 1h at room temperature. The arrows indicate bands corresponding to the activity of the different phosphoglucomutase isoforms.

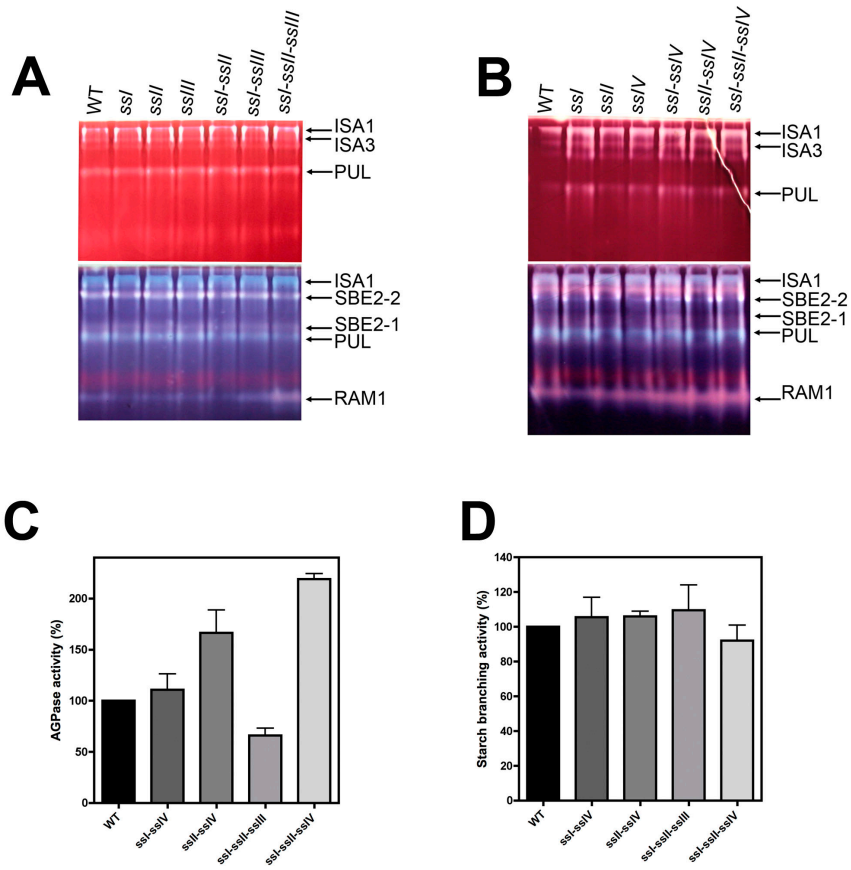

Supplemental Figure 2. Analysis of the activities of starch metabolism enzymes in different *ss* mutant plants. Leaves from three-week-old wild type and *ss* mutant plants were harvested at midday and disrupted using a tissue homogenizer in the presence of 50 mM Hepes, pH 7.6 and proteases inhibitor cocktail. The crude extract was centrifuged for 15 min at 13.000 x g and 4ºC and the supernatant was used to determine the activity of starch metabolism enzymes using *in vitro* or zymograms assays. **A)** Starch modifying activities (hydrolases, branching enzymes) using native PAGE. 100 µg of proteins from crude leaf extracts was loaded onto native PAGE (7.5% acrylamide) containing soluble potato starch (0.3% final concentration). After migration (under native conditions for 3h at 4°C at 15V.cm^{-1}), the gel was incubated overnight at room temperature in the following buffer: Tris/HCl 100 mM pH 7.0, $MgCl_2$ 1 mM, $CaCl_2$ 1 mM, DTT 1 mM. Starch modifying activities were revealed by iodine staining. **B)** Starch debranching activities visualized using native PAGE zymograms. Debranching enzymes were tested on glucan-containing gels as follows: 100 µg of leaf extract proteins was loaded onto a native PAGE (7.5% acrylamide) containing soluble potato starch (Sigma) at 0.3% final concentration and separated for 3 h at 4°C and 15 V.cm^{-1}. The gels were incubated overnight at room temperature in the following buffer: 50 mM sodium citrate pH 6.0, 5 mM DTT, 50 mM Na_2HPO_4. The activities were revealed by soaking the gel in iodine solution (I_2 0.2% w/v and KI 2% w/v).

C) ADP-glucose pyrophosphorylase activities of wild-type and different *ss* mutant plants. Activity was determined in the synthesis direction as described in the Materials and Methods section. **D)** Starch branching activities of wild type and different *ss* mutant plants. Values are expressed as percentage of the respective activity determined for wild-type plants and represent the mean of three independent experiments. Vertical bars: standard error.

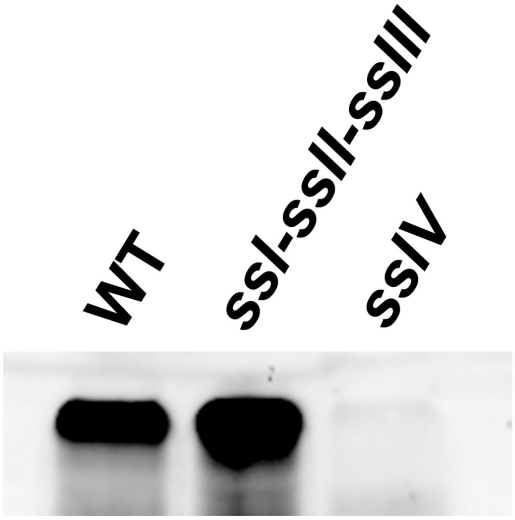

Supplemental Figure 3. Immunoblot analysis of WT, *ssIV* and *ssI-ssII-ssIII* plants using antibody against SSIV protein. Immunoblot analysis of crude leaves extracts from WT*, ssIV* and *ssI-ssII-ssIII* mutant plants. Proteins (25 µg) were separated by SDS-PAGE electrophoresis, transferred to nitrocellulose filters and immunolabelled with rabbit antiserum raised against a 178-amino-acid fragment of the N-terminal region of SSIV protein.

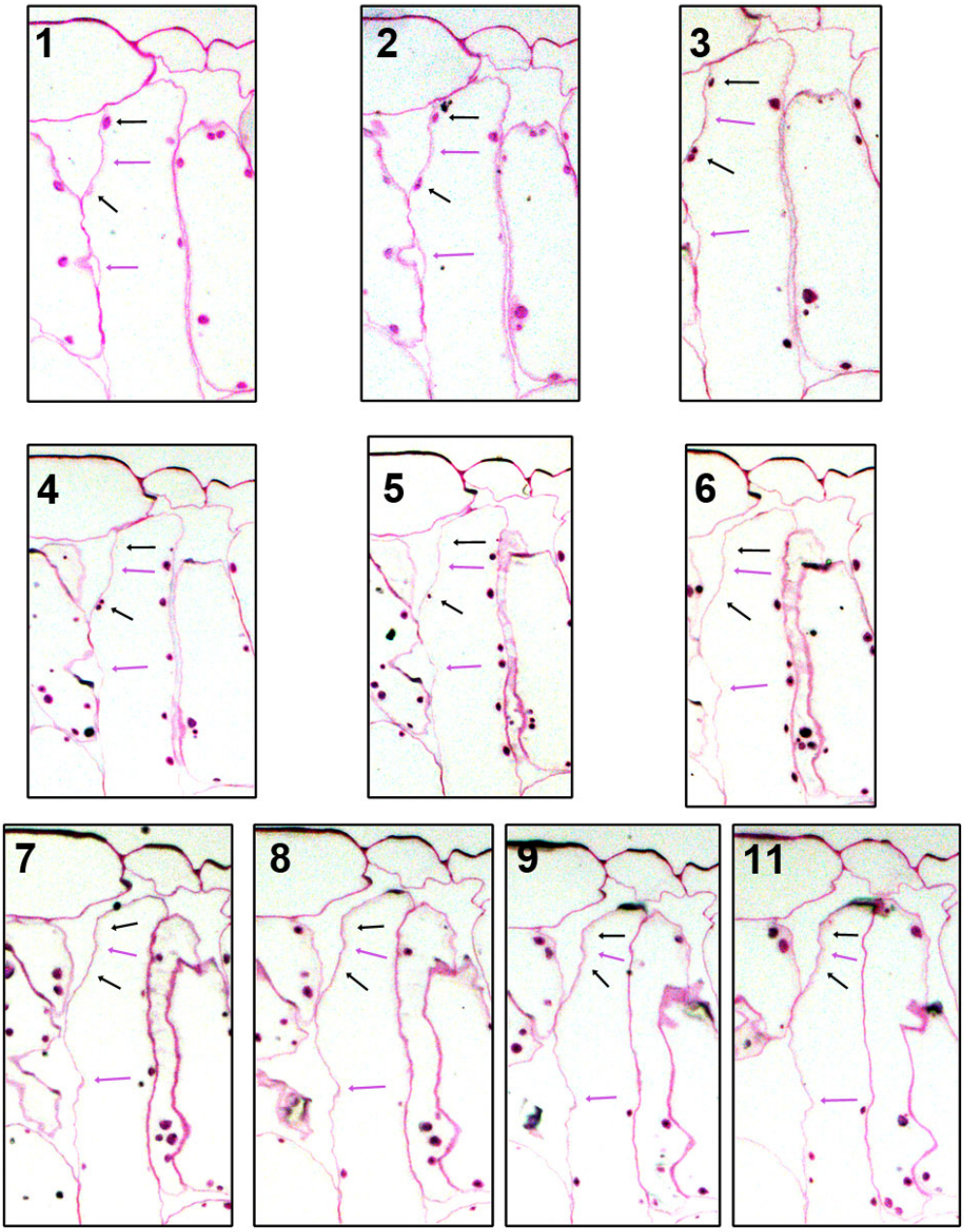

Supplemental Figure 4. **Serial sections of *ssI-ssII-ssIV* triple mutant leaves stained with the periodic acid-Schiff's (PAS) reaction for carbohydrate**. Leaves from three-week-old plant were collected at midday and fixed and embedded as described in the Materials and Methods section. Semi-thin (1 µm) serial sections were stained with the PAS reaction for carbohydrates. The numbers in the panels indicate the order in the sections. The black arrows show starch granules completely dissected along the serial sections, whereas the pink arrows show areas containing chloroplasts without visible starch granules (see **Supplemental Figure 5**).

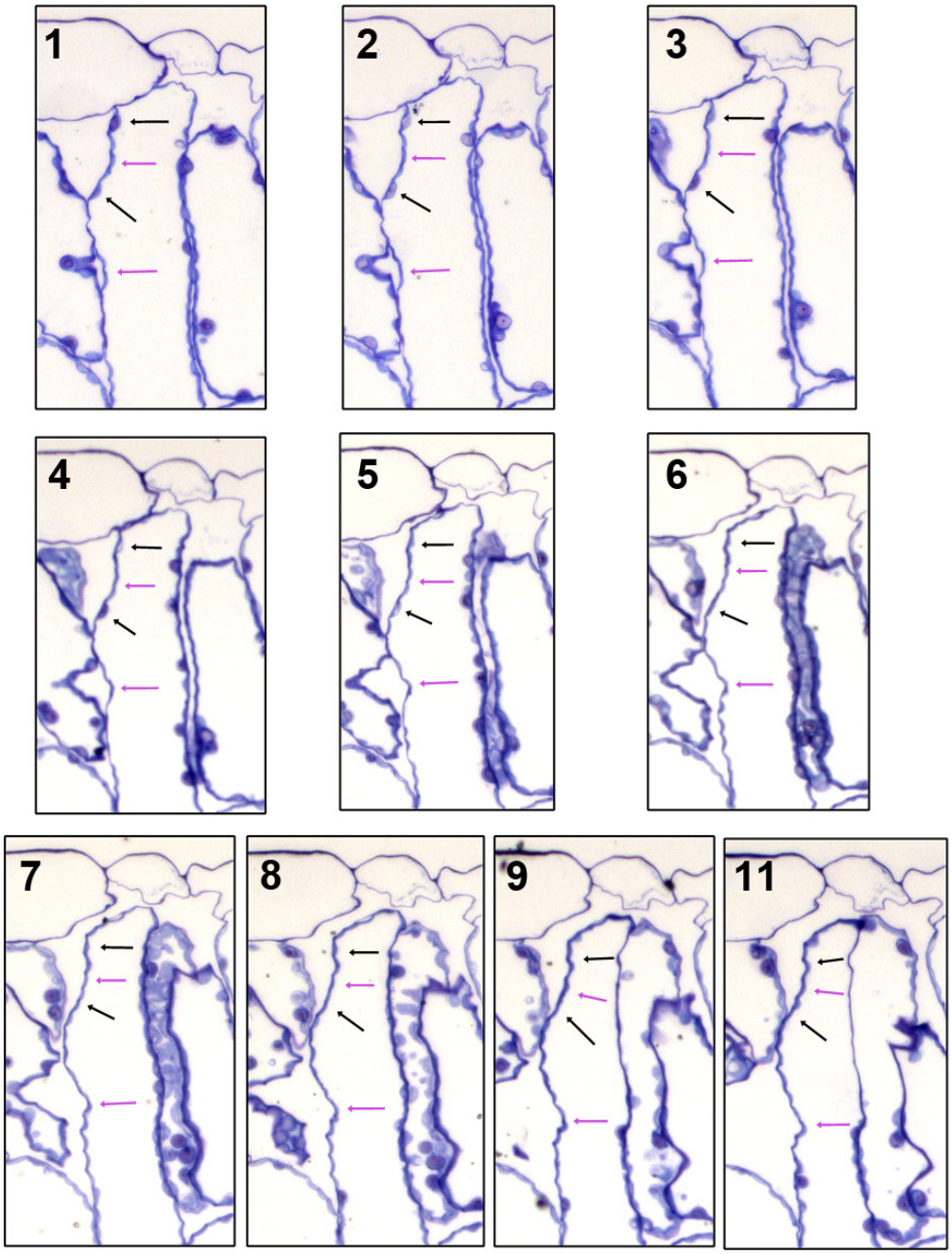

Supplemental Figure 5. **Serial sections of *ssI-ssII-ssIV* triple mutant leaves stained with the PAS reaction for carbohydrates and toluidine blue**. The same sections described in **Supplemental Figure 4** were subsequently stained with toluidine blue in order to show the chloroplasts. The black arrows show starch granules completely dissected along the serial sections, whereas the pink arrows show areas containing chloroplasts without visible starch granules. *Arabidopsis* chloroplasts are lens-shaped, 5-10 μm in diameter and 4μm thick (Mullet, 1988).

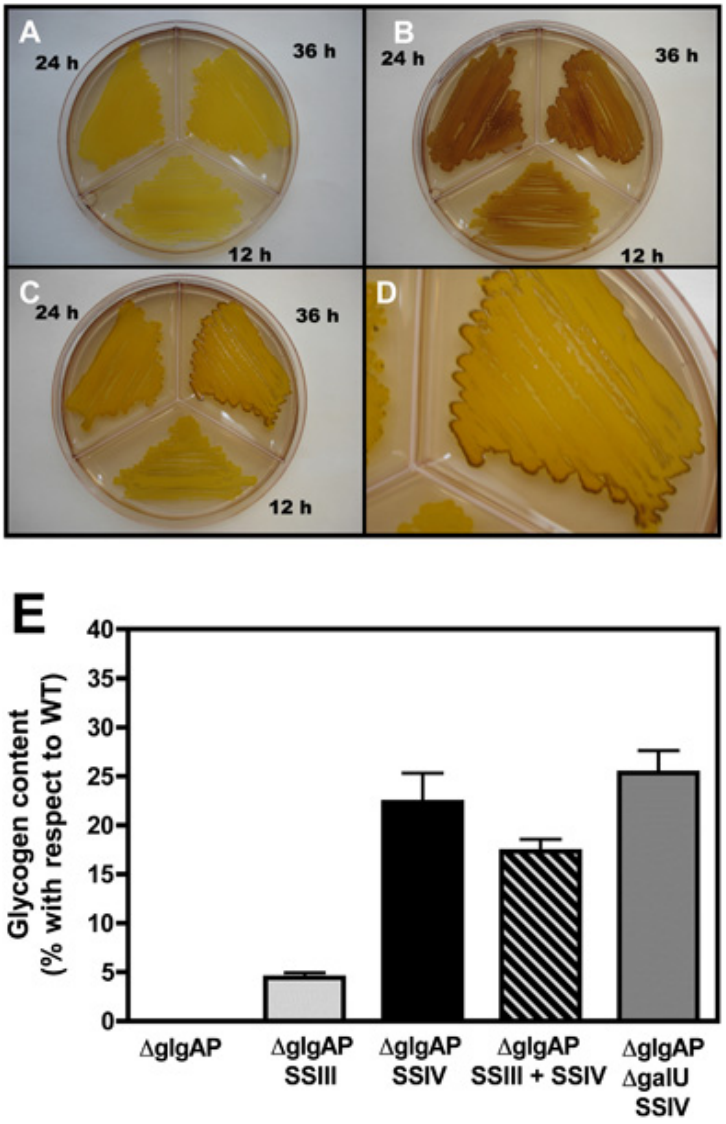

Supplemental Figure 6. SSIII and SSIV expression complement the glycogen-less phenotype of *ΔglgAP E. coli* cells. Iodine staining of (A) *ΔglgAP* cells, (B) *glgA* expressing *ΔglgAP E. coli* cells and (C,D) *SSIV*-expressing *ΔglgAP E. coli* cells after incubation for 12h, 24 h and 36 h of incubation in solid Kornberg medium supplemented with 50 mM glucose. (E) Quantitative measurement of glycogen content in double *ΔglgAP ΔgalU E. coli* cells, *ΔglgAP E. coli* cells and *ΔglgAP E. coli* cells expressing SSIII and/or SSIV.

A

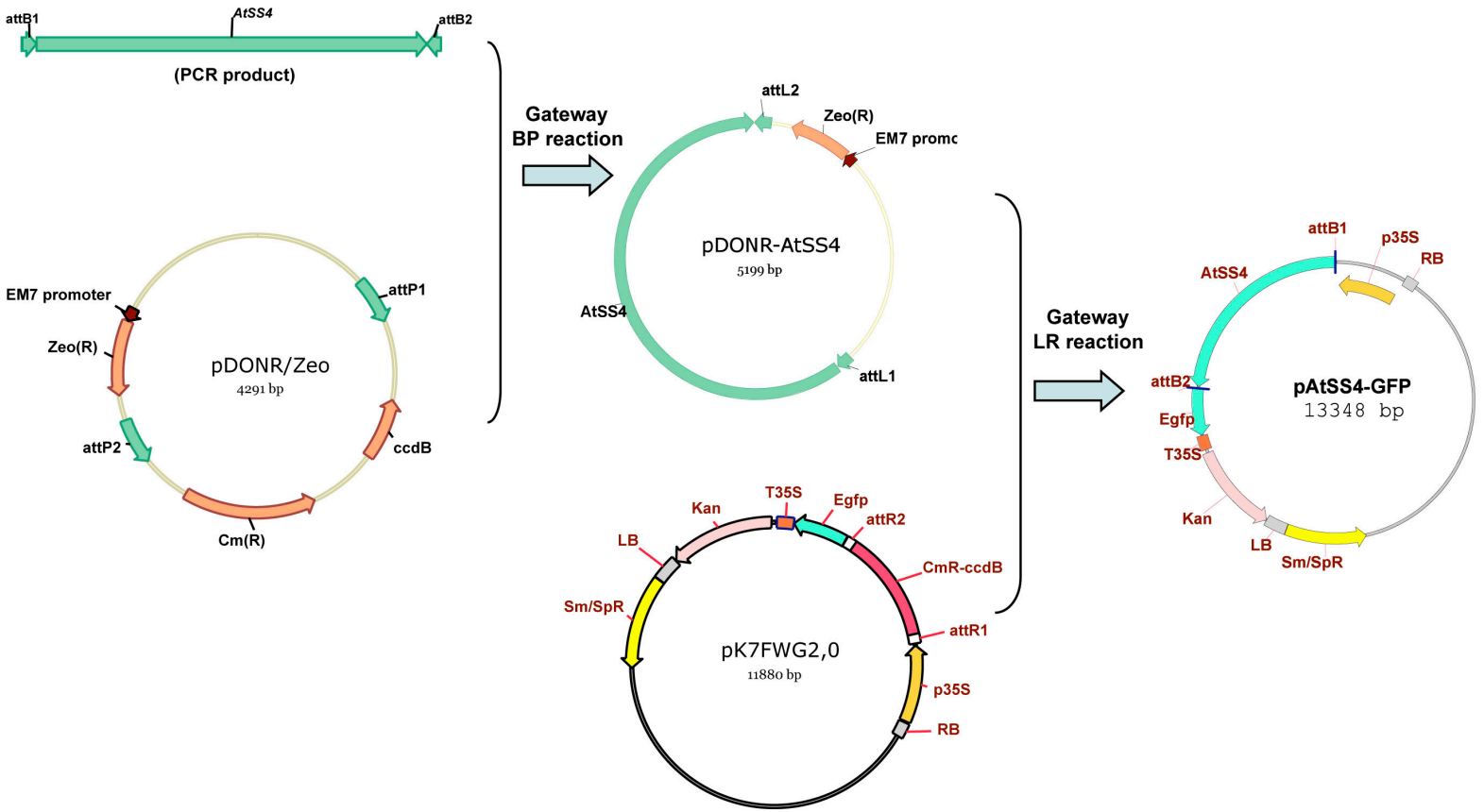
attB1
AtSS4
attB2
(PCR product)
Gateway
BP reaction
attL2
Zeo(R)
EM7 promc
pDONR-AtSS4
5199 bp
AtSS4
attL1
EM7 promoter
Zeo(R)
pDONR/Zeo
4291 bp
attP1
attP2
ccdB
Cm(R)
Gateway
LR reaction
attB1
p35S
RB
AtSS4
attB2
Egfp
T35S
Kan
LB
Sm/SpR
pAtSS4-GFP
13348 bp
T35S
Egfp
Kan
attR2
LB
CmR-ccdB
Sm/SpR
attR1
pK7FWG2,0
11880 bp
p35S
RB

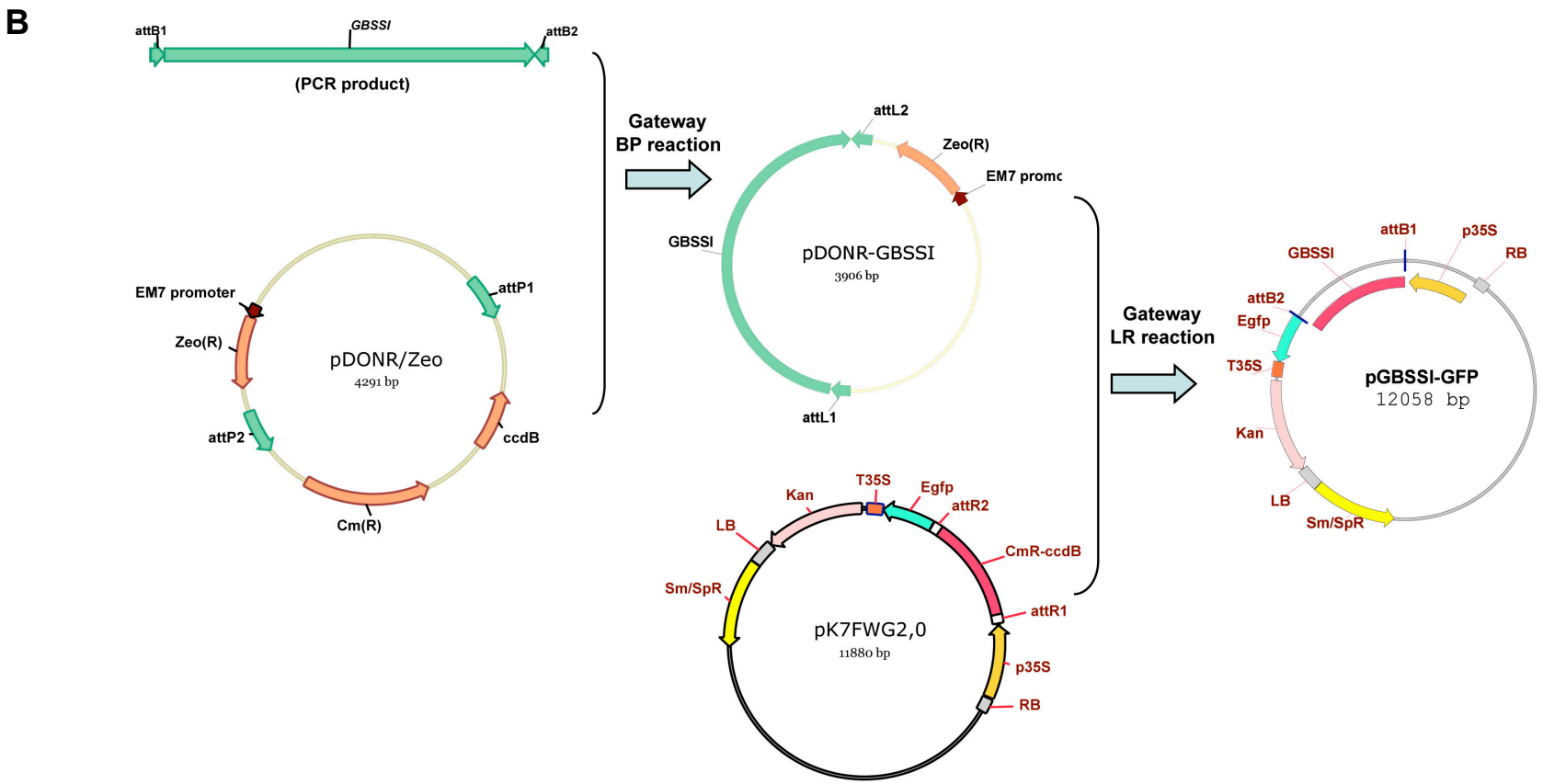

Supplemental Figure 7. Stages required to construct the pSSIV-GFP (**A**) and pGBSSI-GFP (**B**) plasmids necessary to produce plants expressing SSIV and GBSSI fused with GFP, respectively**.**

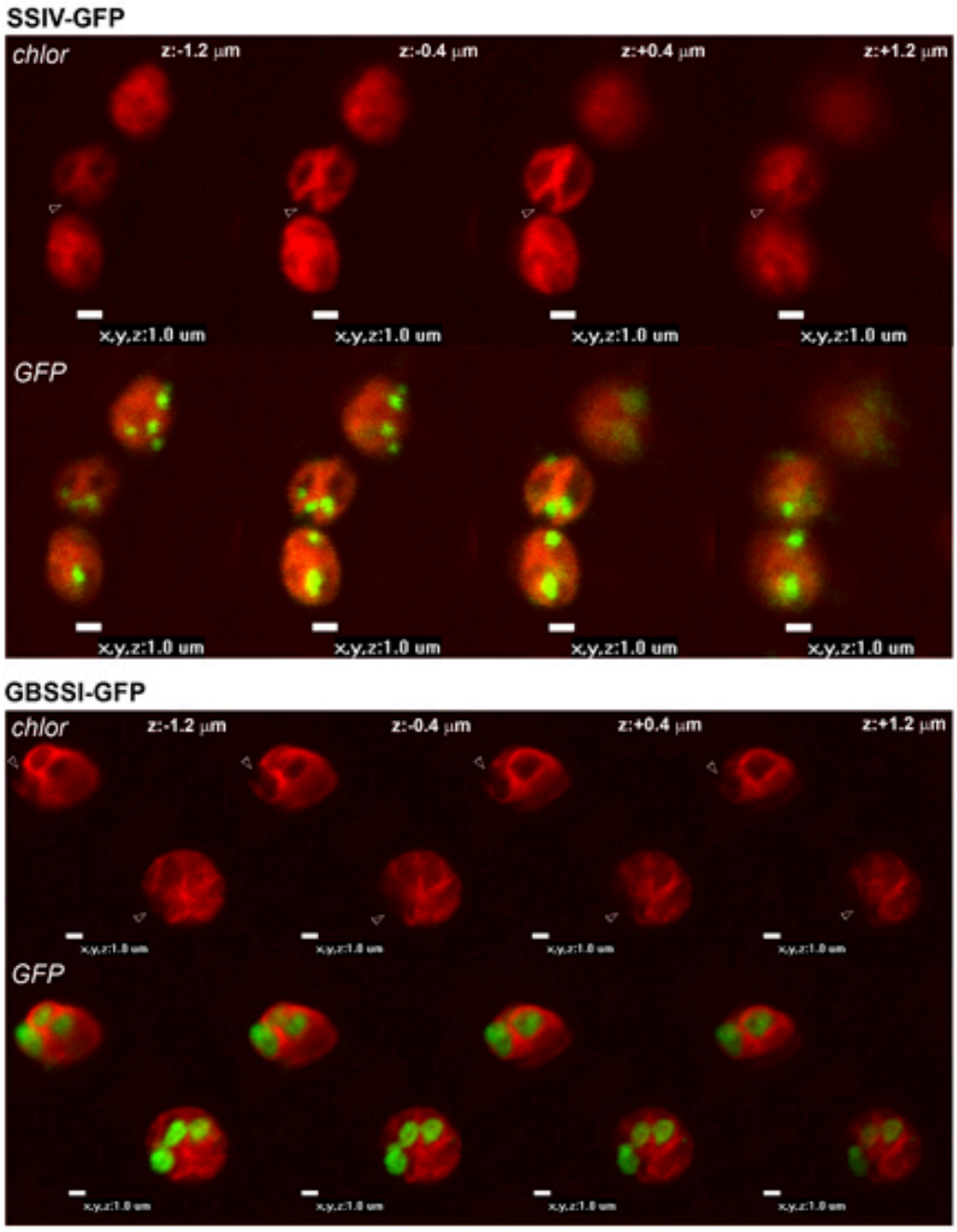

Supplemental Figure 8. Serial analyses of 0.8-μm optical sections of the z-axis capturing SSIV-GFP and GBSSI-GFP fluorescence in *Arabidopsis* chloroplasts. These sections clearly show that GFP fluorescence is mainly associates with the poles of starch granules in SSIV-GFP expressing plants, whereas GFP fluorescence is uniformly distributed within the whole starch granule in GBSSI-GFP expressing plants.

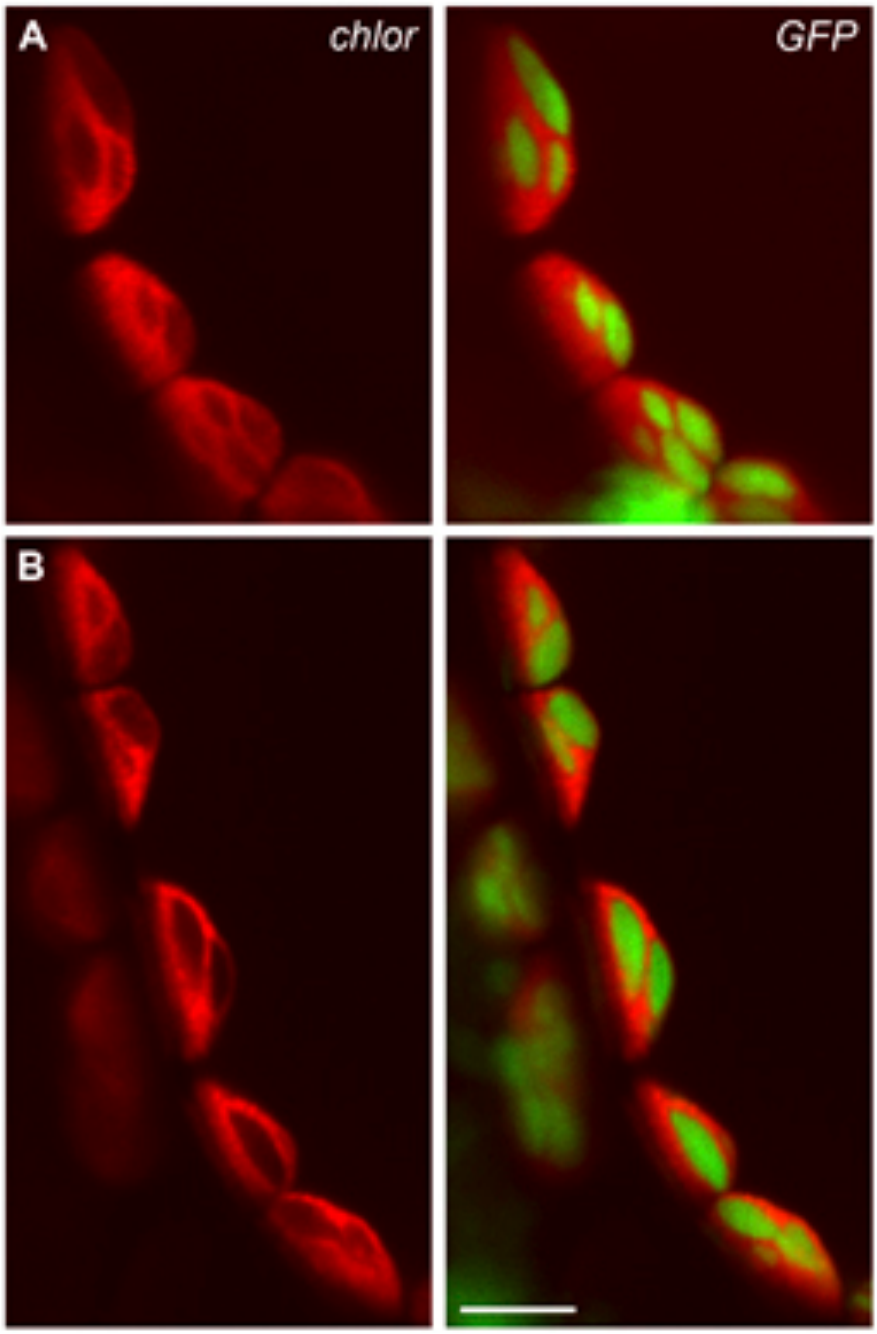

Supplemental Figure 9. Localization of GBSSI-GFP in *Arabidopsis* chloroplasts. Note that GFP fluorescence is uniformly distributed within the oval structures (starch granules) detected in the autofluorescence images (chlor).

Supplemental Table 1. Starch synthase genes, mutant lines and primers used to select mutant alleles.

Gene **AGI code**	**Line identifier/mutation**	**Primers used in this work (5'-3')**	**Ecotype**	**Reference**
SSI At5g24300	Genoplante_203C08/ insertion at intron 1	Fwd: TTTCCGTCCGATCGCCAGTCTC Rev : TACGCCAAAGTCAGCCATTACAA Tag5 (T-DNA) : CTACAAATTGCCTTTTCTTATCGAC	WS	Delvallé et al (2005)
SSII At3g01180	Genoplante_549A11/ insertion at exon 8	Fwd: GGGGACCGGTAGATGATTTC Rev : CGGTCGCCCTGTGCCTAAC Tag5 (T-DNA) : CTACAAATTGCCTTTTCTTATCGAC	WS	Zhang et al. (2008)
SSIII At1g11720	SALK_065732/ insertion at exon 13	Fwd: AAAGGGCACAAGCTCAAGTTC Rev: TCTTGCTCCATCACCGTCTT Lba1 (T-DNA): TGGTTCACGTAGTGGGCCATCG	Col	Zhang et al (2005)
	Genoplante_117H05/ insertion at exon 12	Fwd: ATACGGCGCTGTTCCTGTTGTTA Rev: ATTCATCTTAGAGCTTCCATTTTA Tag5 (T-DNA) : CTACAAATTGCCTTTTCTTATCGAC	WS	This work
SSIV At4g18240	GABI_290D11/ insertion at exon 11	Fwd: CATTGTAACAACCGTGTCCCC Rev: GTTGTTCAATACCTTCAAATTCCC GABI-1 (T-DNA): CCCATTTGGACGTGAATGTAGACAC	Col	Roldán et al. (2007)
	Genoplante_559H08/ insertion at intron 1	Fwd: AACCCATGGATTAGCAGGAA Rev : CAAATGGGAAATGAAAGGAAC Tag5 (T-DNA) : CTACAAATTGCCTTTTCTTATCGAC	WS	Roldán et al. (2007)

Supplemental Table 2: *E. coli* strains and plasmids used in this study

Designation	Relevant genotype	Source
Bacteria		
BL21(DE3)	F^- *ompT gal dcm lon* $hsdS_B(r_B^- m_B^-)$ λ(DE3 [lacI lacUV5-T7 gene 1 ind1 sam7 nin5])	Novagen
BL21(DE3) *ΔglgCAP*	*ΔglgCAP::*Kan^r, complete *glgCAP* operon replaced by a kanamycin resistance cassette	This work
BL21(DE3) *ΔglgAP*	*ΔglgAP::*Kan^r , *glgA and glgP* replaced by a kanamycin resistance cassette	This work
BL21(DE3) *ΔglgCAP ΔgalU*	*ΔglgCAP::*Kan^r, complete *glgCAP* operon replaced by a kanamycin resistance cassette	
	ΔgalU::Sm^r, *galU* replaced by a spectinomycin resistance cassette	This work
Plasmids		
pACYCDuet	Expression plasmid, Cm^r chloramphenicol resistance	Novagen
pACYCDuet-glgA	pACYCDuet directing *glgA* expression	Morán-Zorzano et al. (2007)
pACYCDuet-SS3	pACYCDuet directing *SSIII* expression	This work
pACYCDuet-glgC	pACYCDuet directing *glgC* expression	This work
pET45b	Expression plasmid, ampicillin resistance	Novagen
pET45-SS3	pET45 directing SSIII expression	This work
pET45-SS4	pET45 directing SSIV expression	This work

Supplemental Table 3: Primer pairs for *glgCAP*, *glgAP* and *galU* disruptions. Priming sequences for the kanamycin resistance gene are indicated in bold. Priming sequences for the spectinomycin resistance gene are underlined.

Locus	Primer	Sequence
glgCAP	Forward	5´- GTG CAG CAC ATT CAG CGC GGC TGG TCA TTC TTT AAT GAA GAA ATG AAC GAG TTT GTC GAT **AAA GCC ACG TTG TGT CTC AA** –3´
	Reverse	5´- ATT CGC ACC GTC CAA CGT ACC GAT AGT CAG CGC ACC GTT AAG CGC AAA CTT CAT GTT ACT **GCG CTG AGG TCT GCC TCG TG** –3´
glgAP	Forward	5´-GCG CCG CAT CTC TAT GAT CGT CCG GGA AGC CCG TAT CAC GAT ACC AAC TTA TTT GCC TAT **AAA GCC ACG TTG TGT CTC AA**–3´
	Reverse	5´- ATT CGC ACC GTC CAA CGT ACC GAT AGT CAG CGC ACC GTT AAG CGC AAA CTT CAT GTT ACT **GCG CTG AGG TCT GCC TCG TG** –3´
galU	Forward	5´- GCC GGC GAC GAA AGC CAT CCC GAA AGA GAT GCT GCC ACT TGT CGATAA GCC ATT AAT TCA <u>ACG AAC CCA GTG GAC ATA AGC</u>- 3´
	Reverse	5´- ACC TAA TTT ATT ACC GCA GTC ATG GCT CTT CCC TTT CAT ATG ATA GGC TTC CAC CGT TTC <u>ATG CAT GAT ATA TCT CCC AA</u> -3´